Supporting information for

Flexible high-efficiency CZTSSe solar cells on diverse flexible substrates via an adhesive-bonding transfer method

Jung-Hong Min,[1,2,†] Woo-Lim Jeong,[1,2,†] Kiyoung Kim,[1] Je-Sung Lee,[1] Kyung-Pil Kim,[1] Jihun Kim,[1] Myeng Gil Gang,[3] Chang Woo Hong,[3] Jin Hyeok Kim,[3] and Dong-Seon Lee [1,2,]*

[1] School of Electrical Engineering and Computer Science, Gwangju Institute of Science and Technology, Gwangju 61005, South Korea

[2] Research Institute for Solar and Sustainable Energies, Gwangju Institute of Science and Technology, Gwangju 61005, South Korea

[3] Optoelectronic Convergence Research Center, Department of Materials Science and Engineering Chonnam National University, Gwangju 61186, South Korea

[†] These authors contributed equally to this work.

*** Corresponding author**. Tel.: +82 62 7152248; fax: +82 62 7152204

E-mail: dslee66@gist.ac.kr (D. S. Lee)

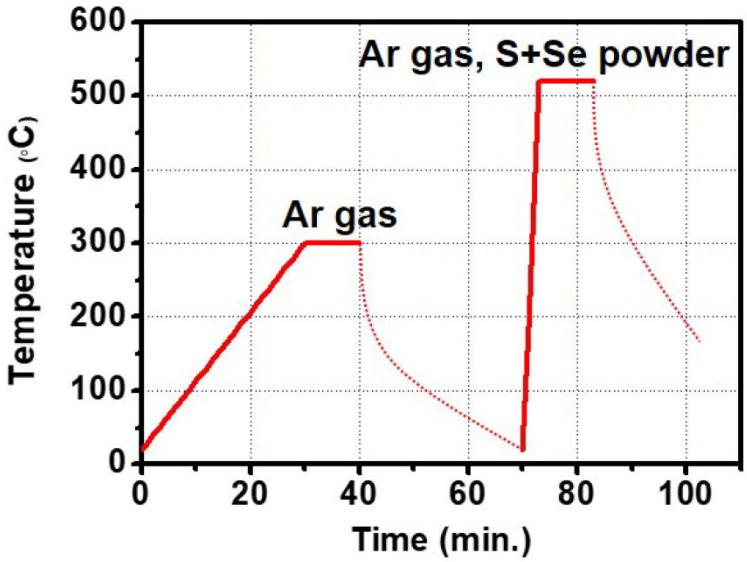

Figure S1. Profiles of temperature and ambient conditions for thermal annealing [1].

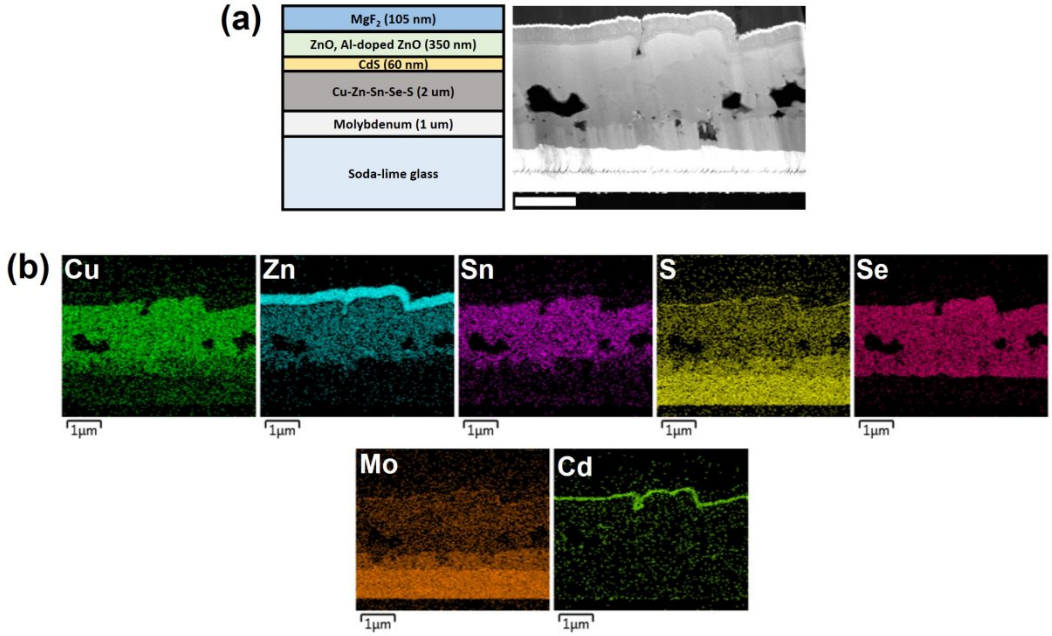

Figure S2. (a) Schematic of CZTSSe solar cell and its TEM image. The scale bar is 1 μm. (b) EDX mapping for TEM related to Cu, Zn, Sn, S, Se, Mo, and Cd.

Table S1. Comparison of the characteristics of some reported flexible CZTSSe solar cells.

Material	Substrate	PCE (%)	Reference
CZTSSe	Mo foil	3.8	[2]
CZTSe	Stainless steel foil	6.1	[3]
CZTS	Stainless steel foil	6.29	[4]
CZTSSe	Mo foil	6.78	[5]
CZTSSe	Mo foil	8.0	[6]
CZTSSe	Mo foil	10.34	[7]
CZTS	Polyimide	0.15	[8]
CZTS	PET	0.83	[9]
CZTSSe	PET	7.1	this work

Table S2. Composition ratio of the CZTSSe absorber measured by EDX [10, 11].

	Chemical composition					Compositional ratio		
	Cu (at%)	Zn (at%)	Sn (at%)	Se (at%)	S (at%)	Cu/ (Zn+Sn)	Zn/Sn	(Se+S)/ Metal
CZTSSe absorber	18	20.1	13.3	34.2	14.4	0.56	1.51	0.95

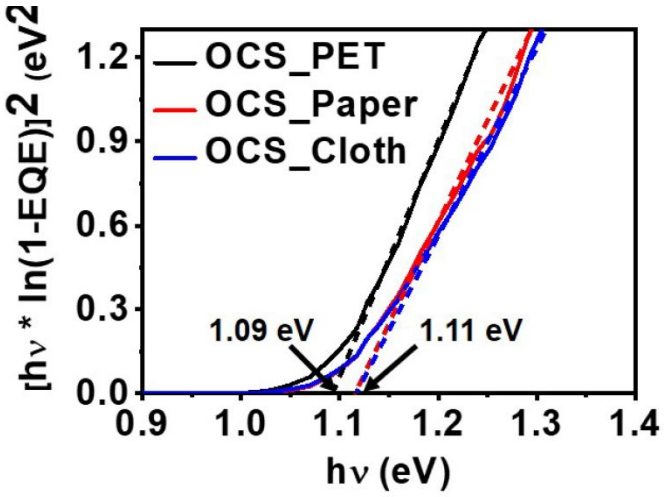

Figure S3. $[h\nu \times \ln(1-EQE)]^2$ vs hυ curves obtained from EQE measurement of the OCSs.

Table S3. Device characteristics of the original CZTSSe solar cells on the soda-lime glasses for all cells.

	V_{oc} (mV)	J_{sc} (mA/cm^2)	FF (%)	η (%)	R_{sh} (Ω cm^2)	R_s (Ω cm^2)
OCS_PET 1	433.6	31.3	58.3	7.9	239.6	2.66
OCS_PET 2	426	34.6	56.4	8.3	266.4	2.67
OCS_PET 3	426	33.6	57.9	8.3	345	2.54
OCS_PET 4	416	30.7	59.6	7.6	169.4	2.41
OCS_PET 5	408.5	31.7	58.6	7.6	139.3	2.44
OCS_PET 6	411.1	31.4	59.2	7.6	179	2.42
OCS_Paper 1	451.1	29.2	54.9	7.2	381	3.23
OCS_Paper 2	441.1	31.8	53.8	7.6	315	3
OCS_Paper 3	436.1	30.5	52.6	7.0	270.5	3.06
OCS_Paper 4	443.6	29.5	51.3	6.7	282.6	3.4
OCS_Paper 5	436.1	31.5	49.4	6.8	227.1	3.43
OCS_Paper 6	223	27.9	31	1.9	11.7	5.1
OCS_Cloth 1	423.5	28.5	53.6	6.5	360	3.42
OCS_Cloth 2	406	29.3	54	6.4	420	3.07
OCS_Cloth 3	406	29.3	54.5	6.5	214.6	2.94
OCS_Cloth 4	411.1	27.3	55.1	6.2	375	3.1
OCS_Cloth 5	403.5	28.2	55.7	6.3	261	2.89
OCS_Cloth 6	403.5	27.6	57.2	6.4	213.7	2.81

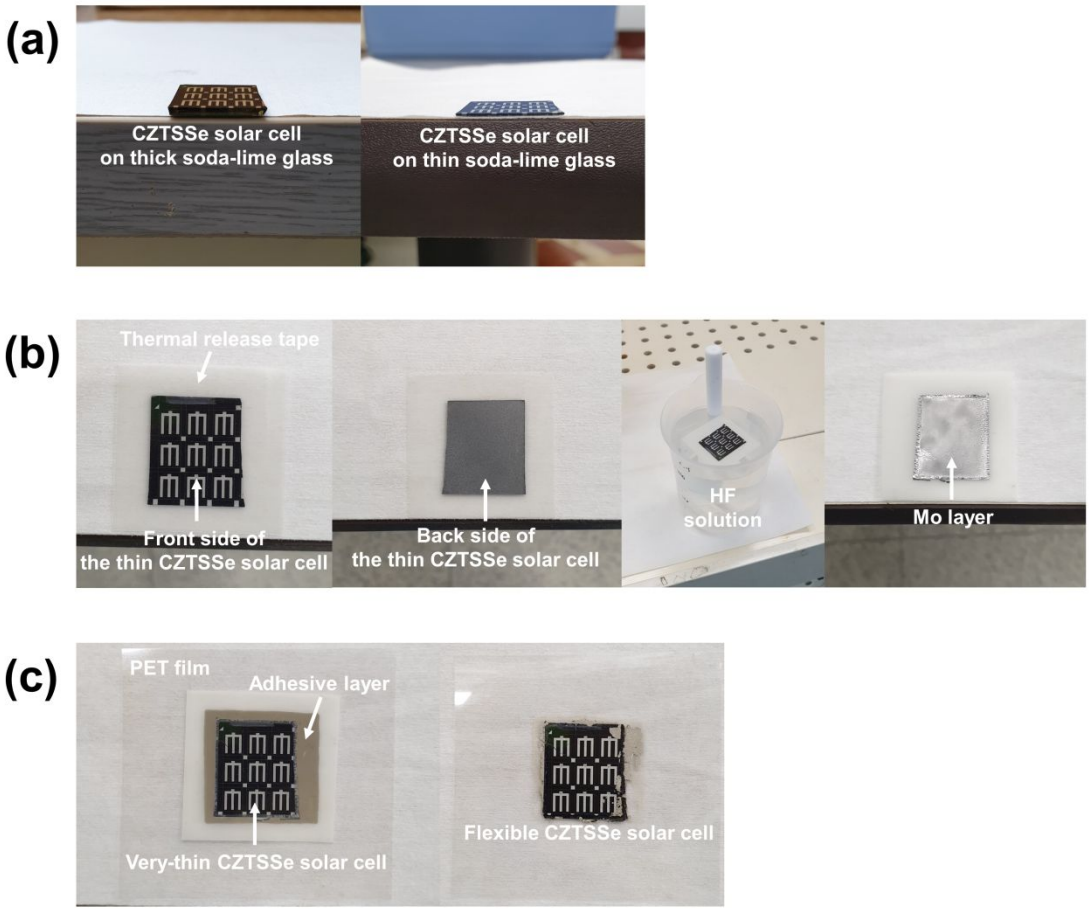

Figure S4. Digital camera images for fabrication process of a flexible CZTSSe solar cell on a PET substrate: (a) Grinding of soda-lime glass. (b) Removing whole soda-lime glass. (c) Transferring the very-thin CZTSSe solar cell on the PET substrate.

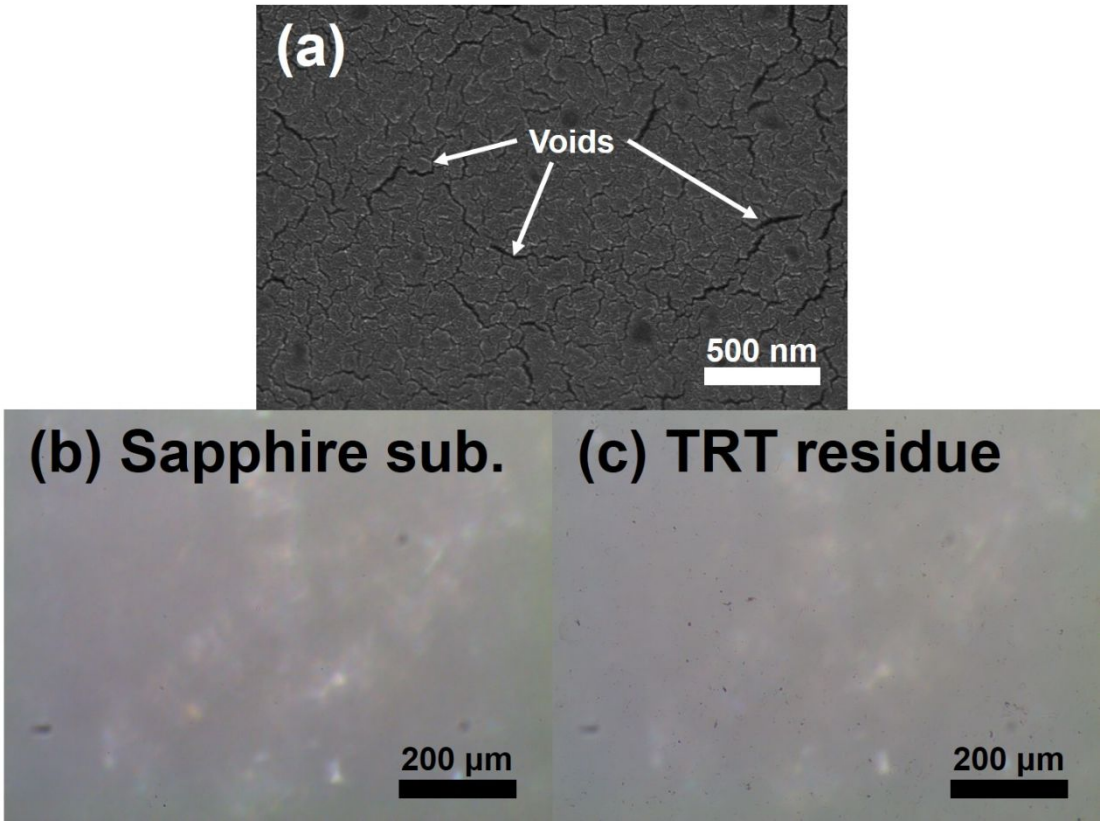

Figure S5. (a) An SEM image of the surface of the thermal release tape (TRT). Optical microscopy images of (b) the transparent sapphire substrate and (c) the TRT residue on it.

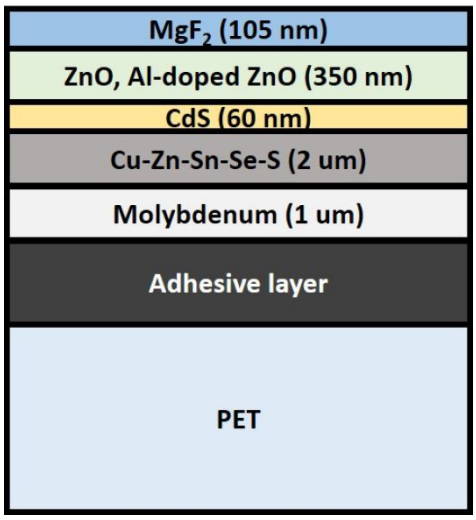

Figure S6. A schematic of the flexible CZTSSe solar cell fabricated on a PET substrate.

Table S4. Device characteristics of the FCSs on various flexible substrates for all cells.

	V_{oc} (mV)	J_{sc} (mA/cm^2)	FF (%)	η (%)	R_{sh} (Ω cm^2)	R_s (Ω cm^2)	η_{FCS}/η_{OCS}
FCS_PET 1	428.6	25.2	49.3	5.3	167.5	4.26	0.67
FCS_PET 2	423.6	28.2	49.8	5.9	176.4	3.35	0.71
FCS_PET 3	416.1	28.4	42.2	5	50.9	4.11	0.60
FCS_PET 4	411.1	24	53	5.2	263.8	3.38	0.68
FCS_PET 5	388.5	26.1	49.2	5	113.6	3.42	0.66
FCS_PET 6	413.6	26.6	51.7	5.7	197.2	3.33	0.75
FCS_Paper 1	448.6	24.6	52.1	5.8	428.3	4.08	0.81
FCS_Paper 2	436.1	27.7	51.7	6.2	251.6	3.49	0.82
FCS_Paper 3	418.6	25.7	50.9	5.5	247.2	3.57	0.79
FCS_Paper 4	436.1	14.9	48.7	3.2	236.8	6.78	0.48
FCS_Paper 5	418.6	26.6	46.8	5.2	152.1	4.23	0.76
FCS_Cloth 1	418.6	26.6	47.1	5.3	159	4.66	0.82
FCS_Cloth 2	406	22.6	51.6	4.7	431.3	4.42	0.73
FCS_Cloth 3	406	24.8	47.7	4.8	90.7	4.32	0.74
FCS_Cloth 4	398.5	9.3	53.2	2	412	8.29	0.32
FCS_Cloth 5	391	12	54.9	2.6	519.2	6.3	0.41
FCS_Cloth 6	401	26.7	53.9	5.8	150.3	3.63	0.91

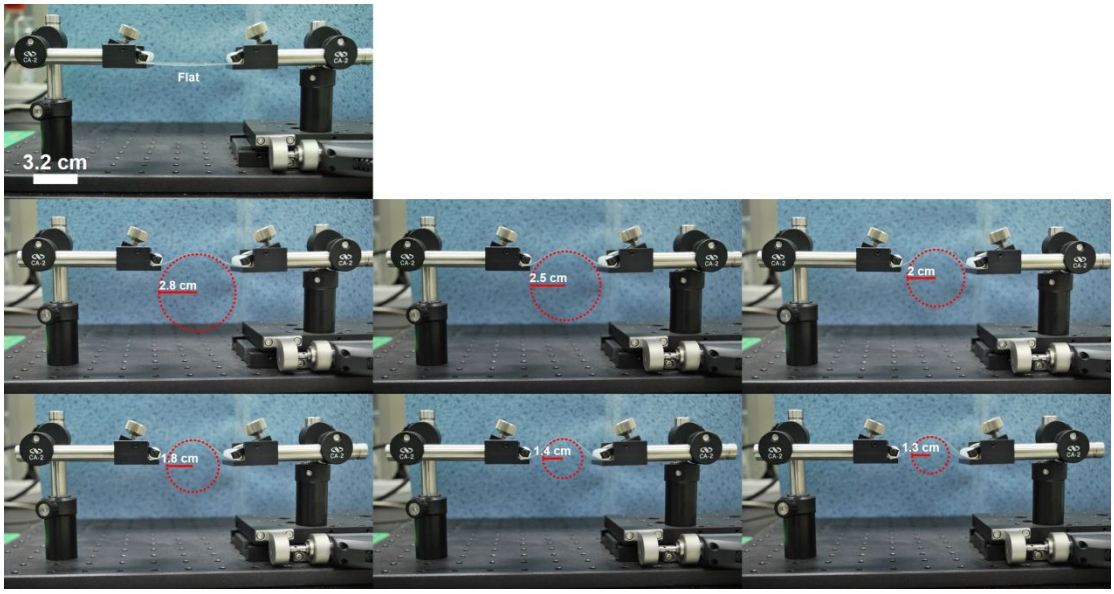

Figure S7. Bending tests by changing the bending radius from 2.8 cm to 1.3 cm.

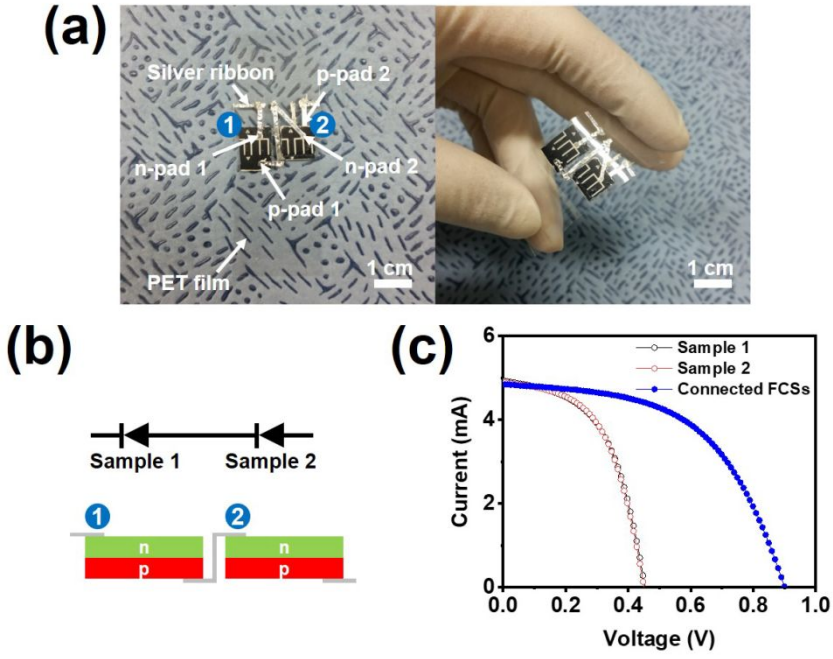

Figure S8. Conveniently connected FCSs: (a) Digital camera images of the conveniently connected FCSs. (b) Schematics of the series-connected solar cells. (c) J-V characteristics for two FCSs and the connected FCSs.

Table S5. Solar cell characteristics of the two FCSs and conveniently connected FCSs.

	V_{oc} (mV)	I_{sc} (mA)	J_{sc} (mA/cm^2)	FF (%)	η (%)	R_{sh} (Ω cm^2)	R_s (Ω cm^2)
Sample 1	457.3	4.9	25.9	52.2	6.18	141.7	4.2
Sample 2	447.2	4.9	25.7	53.9	6.19	172.3	4.47
Connected FCSs	899.5	4.8	12.7	53.6	6.1	787.4	17.13

Table S6. Device characteristics of the extra CZTSSe solar cell sample for all cells.

	V_{oc} (mV)	J_{sc} (mA/cm^2)	FF (%)	η (%)	R_{sh} (Ω cm^2)	R_s (Ω cm^2)	η_{FCS}/η_{OCS}
OCS_PET extra 1	458.7	30.9	54.8	7.8	168.6	3.42	-
OCS_PET extra 2	458.7	32.2	58.4	8.6	224.4	3.05	-
OCS_PET extra 3	458.7	31.3	55.9	8.0	190.1	3.31	-
OCS_PET extra 4	448.6	32	56.3	8.1	211.1	3.21	-
OCS_PET extra 5	463.7	31.4	59.7	8.7	235.8	2.89	-
OCS_PET extra 6	468.7	34.4	57.6	9.3	175.7	2.81	-
FCS_PET extra 1	453.6	28.9	54.3	7.1	106.5	3.29	0.91
FCS_PET extra 2	448.6	26.6	49.7	5.9	102.7	4.85	0.69
FCS_PET extra 3	448.6	27.5	54	6.7	137.4	3.89	0.84
FCS_PET extra 4	443.6	27.1	52.4	6.3	134.8	4.45	0.78
FCS_PET extra 5	453.6	24.9	57.3	6.5	188.4	3.59	0.75
FCS_PET extra 6	453.6	23.8	41.4	4.5	111.7	9.07	0.48

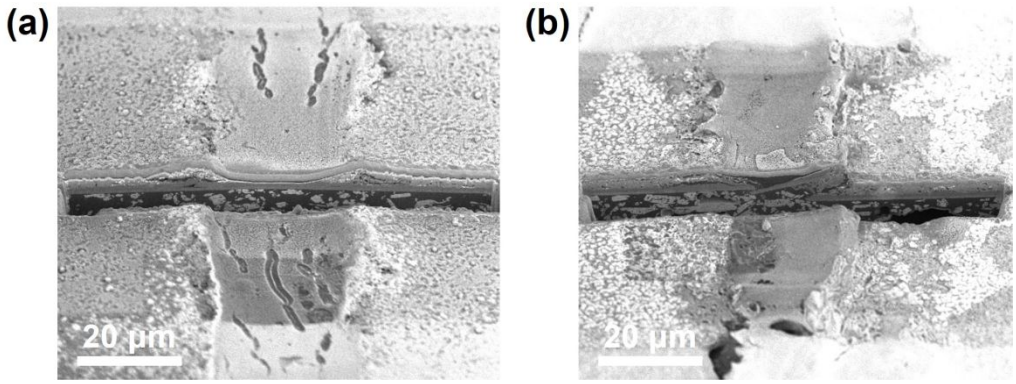

Figure S9. (a) and (b) indicate the zoom-out FIB images for the two boundaries.

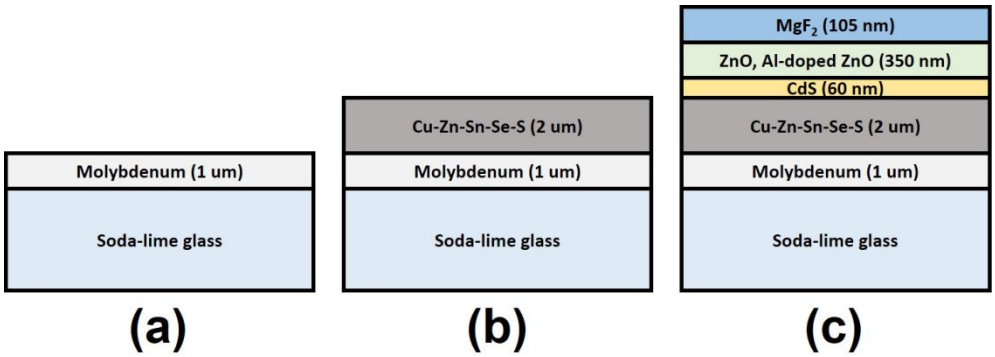

Figure S10. Schematic of each measured layer for nanoindentation [12]. (a) Mo layer on soda-lime glass (Mo layer). (b) CZTSSe absorber on Mo/soda-lime glass (Absorber). (c) CZTSSe solar cell including MgF_2 layer (CZTSSe solar cell).

Table S7. Results of hardness and Young's modulus measured by nanoindentation.

Materials	Hardness (Gpa)	Young's modulus (Gpa)
Razor blade	9.9	223.5
Mo	9.1	162
Absorber	2.3	53
CZTSSe solar cell	4.1	72.8

References

(1) Chen, W.C.; Tunuguntla, V.; Li, H.W.; Chen, C.Y.; Li, S.S.; Hwang, J.S.; Lee, C.H.; Chen, L.C.; Chen, K.H. Fabrication of $Cu_2ZnSnSe_4$ solar cells through multi-step selenization of layered metallic precursor film. *Thin Solid Films* **2016,** 618, 42–49.

(2) Xu, X.; Qu, Y.; Barrioz, V.; Zoppi, G.; Beattie, N.S. Reducing series resistance in $Cu_2ZnSn(S,Se)_4$ nanoparticle ink solar cells on flexible molybdenum foil substrates. *RSC Adv.* **2018**, 8, 3470–3476.

(3) López-Marino, S.; Sánchez, Y.; Espíndola-Rodríguez, M.; Alcobé, X.; Xie, H.; Neuschitzer, M.; Becerril, I.; Giraldo, S.; Dimitrievska, M.; Placidi, M.; Fourdrinier, L.; Izquierdo-Roca, V.; Pérez-Rodríguez, A.; Saucedo, E. Alkali doping strategies for flexible and light-weight $Cu_2ZnSnSe_4$ solar cells. *J. Mater. Chem. A* **2016**, 4, 1895–1907.

(4) Sun, K.; Liu, F.; Huang, J.; Yan, C.; Song, N.; Sun, H.; Xue, C.; Zhang, Y.; Pu, A.; Shen, Y.; Stride, J.A.; Green, M.; Hao, X. Flexible kesterite Cu_2ZnSnS_4 solar cells with sodium-doped molybdenum back contacts on stainless steel substrates. *Sol. Energy Mater. Sol. Cells* **2018**, 182, 14–20.

(5) Yan, Q.; Cheng, S.; Li, H.; Yu, X.; Fu, J.; Tian, Q.; Jia, H.; Wu, S. High flexible $Cu_2ZnSn(S,Se)_4$ solar cells by green solution-process. *Sol. Energy* **2019**, 177, 508–516.

(6) Jo, E.; Gang, M.G.; Shim, H.; Suryawanshi, M.P.; Ghorpade, U.V.; Kim, J.H. 8% efficiency $Cu_2ZnSn(S,Se)_4$ (CZTSSe) thin film solar cells on flexible and lightweight molybdenum foil substrates. *ACS Appl. Mater. Interfaces* **2019**, 11, 23118–23124.

(7) Yang, K.; Kim, S.; Kim, S.; Ahn, K.; Son, D.; Kim, S.; Lee, S.; Kim, Y.; Park, S.; Sung, S.; Kim, D.; Enkhbat, T.; Kim, J.; Jeon, C.; Kang, J. Flexible $Cu_2ZnSn(S,Se)_4$ solar cells with over 10% efficiency and methods of enlarging the cell area. *Nat. Commun.* **2019**, 10, 1–10.

(8) Boshta, M.; Binetti, S.; Donne, A.L.; Gomaa, M; Acciarri, M. A chemical deposition process for low-cost- CZTS solar cell on flexible substrates. *Mater. Tech.* **2016**, 32, 251–255.

(9) Najafi, V.; Kimiagar, S. Cd-free Cu2ZnSnS4 thin film solar cell on a flexible substrate using nano-crystal ink. *Thin solid Films* **2018**, 657, 70–75.

(10) Wang, W.; Winkler, M.T.; Gunawan, O.; Gokmen, T.; Todorov, T.K.; Zhu, Y.; Mitzi, D.B. Device characteristics of CZTSSe thin-film solar cells with 12.6% efficiency. *Adv. Energy Mater.* **2014**, 4, 1301465.

(11) Yang, K.; Son, D.; Sung, S.; Sim, J.; Kim, Y.; Park, S.; Jeon, D.; Kim, J.; Hwang, D.; Jeon, C.; Nam, D.; Cheong, H.; Kang, J.; Kim, D. A band-gap-graded CZTSSe solar cell with 12.3% efficiency. *J. Mater. Chem. A* **2016**, 4, 10151-10158.

(12) Malerba, C.; Valentini, M.; Azanza Rcardo, C.L.; Rinaldi, A.; Cappelletto, E.; Scardi, P.; Mittiga, A. Blistering in Cu_2ZnSnS_4 thin films: correlation with residual stresses. *Mater. Des.* **2016**, 108, 725-735.